

Highly tunable valence-band offset at the (111) Si/Si homojunction via a CaF monolayer saturated with H

S. Picozzi* and S. Massidda

INFM, Dipartimento di Scienze Fisiche, Università degli Studi di Cagliari, 09124 Cagliari, Italy

A. Continenza

INFM, Dipartimento di Fisica, Università degli Studi di L'Aquila, 67010 Coppito, L'Aquila, Italy

R. Resta

INFM, Dipartimento di Fisica Teorica, Università di Trieste, Strada Costiera 11, I-34014 Trieste, Italy

(Received 16 December 1996)

The possibility of modifying the band lineup at semiconductor heterojunctions by deposition of intralayers of different materials is becoming a tool in “band engineering.” It was found that CaF_2 , when inserted between Si (111) and *a*-Si, generates a huge band offset. We present first-principles calculations for a similar system, where *a*-Si is replaced by crystalline Si, and the dangling bonds are saturated with H, in two different structural morphologies, with an abrupt interface configuration. We vary the width of the Si bulk layer and relax the positions of the interface atoms. Our results indicate the strong sensitivity of the offset to the interface geometry: the potential lineup varies by as much as 1.5 eV as the interface atoms are relaxed to their equilibrium positions or the interface morphology is changed. [S0163-1829(97)02424-7]

I. INTRODUCTION

The control of band lineups at semiconductors heterojunctions is one of the most interesting challenges in interface physics and is greatly stimulated by the important technological applications that would arise from a full theoretical understanding of the charge readjustment at the interface region. In this context, intralayer deposition has been proposed as an additional degree of freedom in band offset tuning, in order to modify the discontinuity at heterojunctions,¹⁻⁵ as well as to create an artificial misalignment at semiconductor homojunctions.⁶⁻⁸ Dell’Orto *et al.*⁹ used synchrotron radiation photoemission spectroscopy in order to determine the valence-band offset induced at a Si(111)-(*a*-Si) homojunction by deposition of a CaF_2 intralayer: they find a very large effect, the misalignment being of 0.35 eV.

The $\text{CaF}_2/\text{Si}(111)$ isolated interface has been the object of several previous investigations. The small lattice mismatch (0.6%), which allows the pseudomorphic growth of CaF_2 films on Si substrates, has stimulated great theoretical¹⁰⁻¹² and experimental¹³⁻¹⁶ interest for this ionic/covalent interface, also proposed as a good candidate for microelectronic and optoelectronic devices.¹⁷

Stimulated by the experimental results, we performed full-potential linearized augmented plane-wave (FLAPW) calculations for several superlattices (SL’s), in which a calcium fluoride monolayer is inserted in a bulk Si crystal normally to the [111] direction, focusing on the dependence of the valence-band offset (VBO) on the interface morphology. Experimental evidence (see Ref. 9 and references therein) indicates that a dissociation reaction transforms CaF_2 in a CaF monolayer and that intermixing processes during the interface formation can be completely ruled out. On the basis of previous work,^{11,12} we also know that the CaF layer grows by forming a strong Si-Ca bond with the Si(111) substrate.

Unfortunately, there is no experimental or theoretical clue about the microscopic morphology of the F-Si junction on the other side of the intralayer. Despite the small lattice mismatch, an ideal (i.e., crystalline and defect-free) junction must be ruled out on the basis of bond-counting arguments: at the real junction, dangling bonds must be saturated by some kinds of defects and/or reconstruction. The only existing measurement refers to the case where the intralayer joins to *amorphous* Si, and furthermore nothing is known about the dependence of the measured effect upon growth conditions. Given the above, guessing a microscopic morphology that is accurately representative of the experiment is a very hard, if not impossible, task: the aim of this work is therefore different. We content ourselves with speculating about a few simple morphologies, each of them being compatible with the interface chemistry, but none of them being indeed trustworthy as a realistic one. We will demonstrate that the (largely arbitrary) choice of the microscopic morphology has huge effects on the calculated band offset in this system. Our specific choice in this work is to replace the *a*-Si overlayer of the real experiment with a crystalline (111) overlayer, and to saturate its dangling bonds with H atoms. We therefore considered abrupt interface configurations of the type Si-Ca-F-H-Si: our computational structure is indeed a Si/CaFH/Si superlattice.

We first start with “ideal” geometries, obtained using the very similar Si and CaF_2 bond lengths. We then allow for structural relaxation (which turns out to be as large as 20% of the bulk bond lengths) and compare the results obtained in the two cases. We consider two different structural arrangements, which differ noticeably in the morphology of the Si layers grown on top of the CaF intralayer. We find that in these systems the VBO is strongly affected by the interface morphology and may vary by as much as 1.5 eV. The experimental figure of Ref. 9 is within our variation range. We

suggest that variation of the growth conditions should strongly affect the measured band offset.

This paper is organized as follows: after a brief description of some computational details (Sec. II), we discuss results concerning the structural properties (Sec. III) and the valence-band offset (Sec. IV) of the various interfaces considered. Finally, in Sec. V we draw our conclusions.

II. TECHNICAL DETAILS

The electronic properties of the structures have been obtained using the density functional formalism, within the local density approximation (LDA). We used the all-electron FLAPW method,¹⁸ with the exchange and correlation as parametrized by Hedin and Lundqvist.¹⁹ Angular momenta up to $l_{\max}=6$ in the muffin-tin spheres ($R_{\text{Ca}}=2.4$ a.u., $R_{\text{Si}}=R_{\text{F}}=2.0$ a.u., and $R_{\text{H}}=0.9$ a.u.) and plane waves with wave vector up to $K_{\max}=3.0$ a.u. were used in the calculations, leading to about 1000 basis functions. The integration over the Brillouin zone has been performed using three special \mathbf{k} points for the hexagonal Brillouin zone of the supercell.²⁰

Atomic relaxations have been calculated making use of the *ab initio* atomic forces, where the Pulay contribution (accounting for the incompleteness of the basis set) is included in the Hellmann-Feynman forces.^{21,22}

III. STRUCTURAL PROPERTIES

Several structural models have been suggested for the Si/CaF₂ interface,¹⁰ but many recent experimental works agree on the fact that CaF is adsorbed on Si on threefold hollow sites (*T4/H3*),^{14,15,23} with strong and limited interactions of Si with Ca and F, respectively. According to this model, we considered two types of interfaces (shown in Fig. 1 and denoted by type A and type B), represented by unit cells with 22 and 18 atoms with hexagonal symmetry. In both cases each unit cell contains two CaF dipole layers, oppositely directed; owing to this geometry, it is possible to unambiguously define two Si bulk regions, delimited by Ca and F atoms, respectively, which allow us to evaluate the VBO. Concerning the dimensions of the supercells used, we checked it by performing calculations for a type B larger cell (with 24 atoms per unit cell) and found that both the 22- and 18-atom cells are thick enough to recover bulk conditions half-way from the interface.

The positions of Ca atoms bound to the silicon substrate and forming an ordered CaF monolayer are common to the two types A and B of interface. However, the two structures differ, except for in the total number of Si atoms, for the positions in the layers above the CaF: the Si atoms of the second layer (indicated by arrows in Fig. 1 and denoted in the following by Si_{II}^{ov}) of the type A interface are on top of Ca, whereas they are above F in the type B interface. This leads to a 120° rotation of the Si hexagons in the region between the two symmetric interfaces and, therefore, to different distances of the overlayer Si atoms from the Ca and F atoms. Since the mismatch is small, we started, as a reference structure, from an unrelaxed structure where all the distances are set equal to the bulk Si interatomic distance. In the unrelaxed type A unit cell, the distance Si_{II}^{ov}-Ca is 3.13 Å and

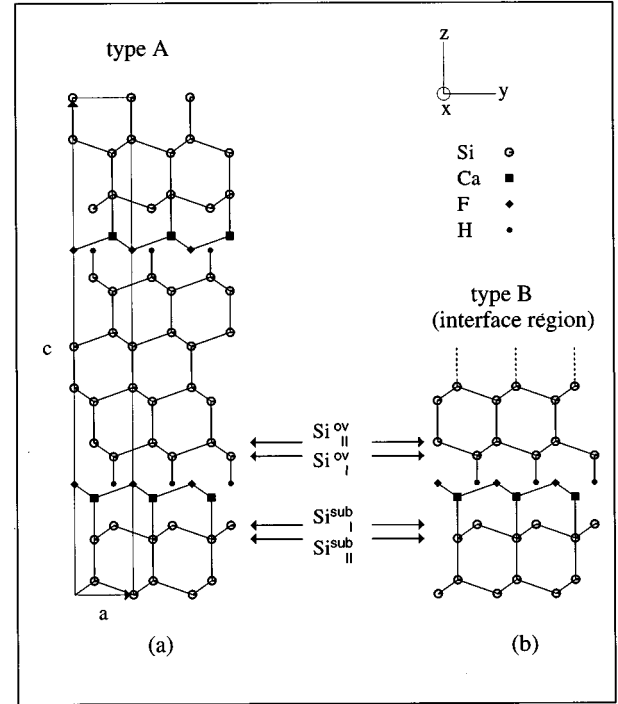


FIG. 1. Unit cell of the unrelaxed structures considered, projected on a vertical plane along the [111] direction: (a) type A and (b) type B.

the distance Si_{II}^{ov}-F is 3.23 Å, whereas in a type B unit cell the distance Si_{II}^{ov}-Ca is 3.84 Å and the distance Si_{II}^{ov}-F is 2.35 Å. Then we allow for relaxation of the atomic positions belonging to the following layers: Ca, F, Si_I^{sub}, Si_{II}^{sub}, Si_I^{ov}, Si_{II}^{ov} (see Fig. 1). Atoms were displaced only along the [111] ordering axis (or, equivalently, along the z direction of Fig. 1), until the calculated atomic forces vanish. Total energy results indicate that the structural configuration of a type A unit cell is favored, by ≈ 0.2 eV/atom, against a type B unit cell, both in the unrelaxed and relaxed cases.

The most important structural parameters obtained by structural minimization are reported in Table I. The relaxed geometries turn out to be radically different from the ideal ones: for example, the distances between the Si surface atoms (Si_I^{sub} and Si_{II}^{sub}) and the Ca atom is increased by as much as 20%. Therefore, even though the CaF₂ and the Si crystals are almost perfectly matched, the abrupt interface is not stable within the ideal lattice structure. In fact, what probably happens at the interface is the formation of a monolayer of CaSi₂, as proposed by experimental¹⁴ and theoretical¹¹ results obtained for the Si/CaF₂ interface. This is in perfect agreement with our results: the distances obtained in this work, 3.20 Å for Si_I^{sub}-Ca and 2.98 Å for Si_{II}^{sub}-Ca, are similar to the SiCa bond length in CaSi₂ (3.03–3.06 Å). Furthermore, the calculated distance ($d_z=2.64$ Å) along the growth direction between the Ca atom and the center of the outer Si double layer (i.e., Si_I^{sub} and Si_{II}^{sub}) is in reasonable agreement with experimental results ($d_z=2.71$ Å), obtained by x-ray reflectivity and transmission electron microscopy.¹⁵ Further confidence in our results comes from the calculated relaxed CaF bond length (2.44 Å), which is slightly bigger than the bulk CaF₂ distance (2.36 Å), as con-

TABLE I. Structural parameters for the systems considered (values in Å).

Distance	Type A		Type B	
	Unrelaxed	Relaxed	Unrelaxed	Relaxed
$\text{Si}^{\text{bulk}}-\text{Si}^{\text{bulk}}$	2.35	2.35	2.35	2.35
$\text{Si}_I^{\text{sub}}-\text{Ca}$	2.71	3.20	2.71	3.20
$\text{Si}_{II}^{\text{sub}}-\text{Ca}$	2.35	2.98	2.35	2.98
Ca-F	2.35	2.44	2.35	2.44
Ca-H	2.36	2.73	2.36	2.73
$\text{Si}_I^{\text{ov}}-\text{H}$	1.54	1.57	1.54	1.57
Ca- $\text{Si}_{II}^{\text{ov}}$	3.13	3.80	3.84	3.86

firmed by the experimental results of Lucas, Wong, and Loretto,¹⁵ who attribute the longer bond length in CaF to the different Ca valence state (+1 in CaF and +2 in CaF₂). To the best of our knowledge, there are no experimental data regarding the Si overlayer, since it grows experimentally as amorphous Si.

IV. VALENCE-BAND OFFSET

The VBO was obtained using a widely adopted method in all-electron calculations,^{24–26} which closely parallels the real x-ray photoelectron spectroscopy (XPS) experiments.^{9,27} The procedure is based on atomic core levels (in particular the Si 1s core levels) as reference energies. Previous theoretical results for different systems²⁸ showed that this method gives VBO values extremely close (within 0.04 eV) to those obtained following the method proposed by Baldereschi *et al.*^{29,3} and largely used in *ab initio* calculations, based on the macroscopic average of the electrostatic potential. Since we are dealing with an intralayer between two slabs of the same semiconductor, the difference between the Si core-level energies on the two sides of the interface (sufficiently far from the CaF monolayer to recover Si bulk conditions) gives directly the VBO. In order to illustrate this procedure, we show in Figs. 2(a) and 2(b) the core levels for the type A unrelaxed and relaxed interfaces, respectively, and we have indicated how the potential lineup is estimated in the two cases. We define the VBO referring to the valence-band top of the Si overlayer so that the VBO will be positive if the valence-band maximum in the Si substrate is at a higher energy than in the Si overlayer.

The VBO's calculated for all the structures considered are reported in Table II. We checked that convergence of the VBO as a function of the cell dimension was reached: we evaluated the VBO for smaller and larger supercells (from 18 to 24 atoms) and found equal values to those shown in Table II within 0.02 eV. Our results clearly show the strong sensitivity of the VBO to the interface morphology, which modifies the charge readjustment and by such means dominates the potential lineup. Let us first discuss the results obtained for the unrelaxed structures. We plot in Fig. 3(a) the macroscopic averages³ of the charge density, $\bar{n}(z)$, for type A (dotted line) and type B (solid line) unrelaxed interfaces, in a region around the interface. The two quantities seem to have an almost identical profile. This similarity, however, is completely overruled by the solution of the Poisson equation: the resulting VBO's, $\Delta V_A^{\text{unr}} = +0.08$ eV and $\Delta V_B^{\text{unr}} = -0.57$ eV,

differ by as much as 0.65 eV (see Table II). Here and in the following the superscript unr (rel) refers to unrelaxed (relaxed) structures.

In order to explain the strong dependence of the potential lineup on the interface morphology, we report in Fig. 3(b) the difference between the macroscopic averages of the charge density [$\Delta\bar{n}(z) = \bar{n}_A^{\text{unr}}(z) - \bar{n}_B^{\text{unr}}(z)$], plotted in the first half of the unit cell. In a type B unit cell, the F atoms show a small charge depletion; at the same time, the Si bonds just on top the interface (i.e., between Si_I^{ov} and $\text{Si}_{II}^{\text{ov}}$ in Fig. 1) show a charge accumulation. The reason for this behavior is

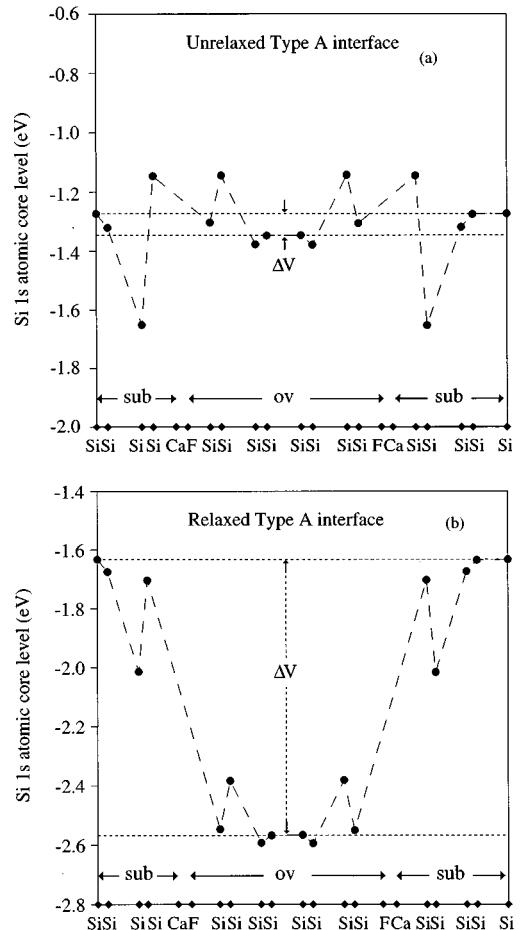


FIG. 2. 1s Si core level energies in the unrelaxed [panel (a)] and relaxed [panel (b)] type A unit cell. The energy scale (in eV) refers to an arbitrary zero.

TABLE II. Valence-band offset (in eV) for the unrelaxed (ΔV^{unr}) and the relaxed (ΔV^{rel}) structures considered.

Type A		Type B	
ΔV^{unr}	ΔV^{rel}	ΔV^{unr}	ΔV^{rel}
+0.08	+0.95	-0.57	+0.67

the presence in a type *B* cell of F-Si_{II}^{ov} bonds along the *c* axis. These bonds mix filled F and empty Si states, drawing charge away from the F layers. The lineup is related to the dipole moment of the charge profile through the relationship³

$$\Delta V = \frac{4\pi}{A} \int zn(z)dz, \quad (1)$$

where *A* is the unit-cell basis area. It is therefore immediately clear that the very small charge transfer far from the interface, shown in Fig. 3(b), can produce an appreciable change of the VBO. In fact, the band-offset problem is dominated by very tiny charge transfers.

Let us examine now how atomic relaxation affects the potential lineup. We note from Table II that the VBO values obtained with the interface atoms in their equilibrium positions differ quite substantially (by as much as 0.87 and 1.24 eV in type *A* and type *B* interfaces, respectively). In the type *B* case, atomic relaxation leads to a VBO ($\Delta V_B^{\text{rel}} = +0.67$ eV), which even has a reverse sign with respect to its value for the unrelaxed case ($\Delta V_B^{\text{unr}} = -0.57$ eV). This can be explained through a simple electrostatic model, which considers the different atomic planes perpendicular to the growth direction as charged planes. We introduce the Born effective charges (e^*), defined as the dipoles linearly induced by unitary displacements of a single ion in an otherwise perfect crystal, and related to the total macroscopic polarization induced by a zone-center phonon with zero electric field boundary conditions. An atomic plane, containing the atomic species *M*, and positioned at z_M , will correspond to an average effective surface charge density $\sigma_M = e_M^*/A$.

Now, at the interface we have successive planes of Si-Ca-F-H-Si, so that we should consider effective charge densities for all of the atomic species involved. However, the SiH bond is strongly covalent and essentially nonpolar. One can then reasonably assume that both the effective charges of H and of its neighboring Si vanish: the substrate and intralayer atoms are mostly responsible for the VBO variation under atomic displacements. We therefore consider our interface region as three parallel charged planes located at $z_{\text{Si}_1^{\text{sub}}}$, z_{Ca} , and z_{F} , with charge densities $\sigma_{\text{Si}_1^{\text{sub}}}$, σ_{Ca} , and σ_{F} , respectively. As a result, we will have two competing double layers or, equivalently, two dipolar distributions: the first one, directed from the substrate to the overlayer [i.e., from the Si₁^{sub} (-) to the Ca (+) atom] and the second one, with opposite sign [i.e., from the F (-) to the Ca (+) atom]. Each of these two double layers will give rise to a potential discontinuity $\Delta V = 4\pi\sigma d/\epsilon$, where *d* is the distance along the growth direction between the oppositely charged planes and ϵ the static dielectric constant of the material. We can therefore express the VBO as the sum of two different dipolar distributions. In particular, if we denote $d_1 = z_{\text{Ca}} - z_{\text{Si}_1^{\text{sub}}}$,

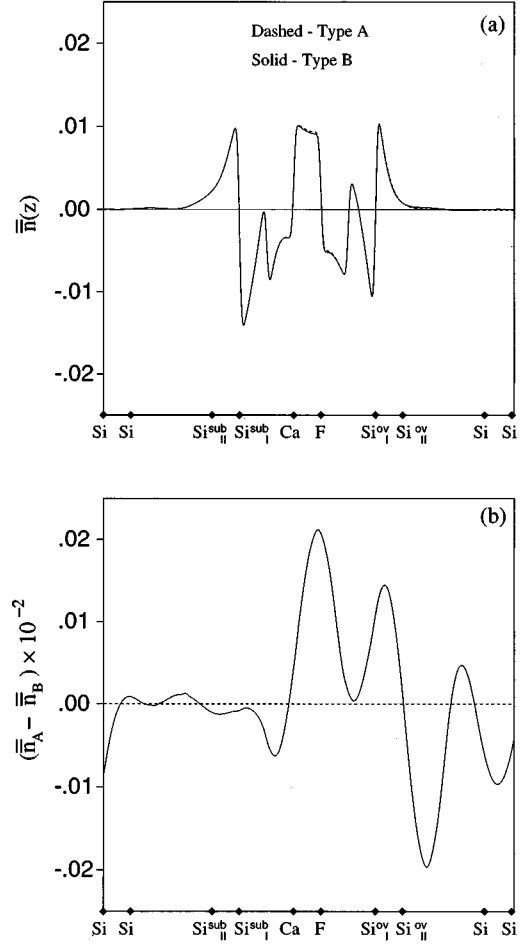


FIG. 3. (a) Macroscopic average of the valence charge density for the unrelaxed structures, plotted in the first half of the unit cell; the dashed (solid) line indicates a type *A* (*B*) unit cell. (b) Difference of the charge density macroscopic average [$\bar{n}_A(z) - \bar{n}_B(z)$] for the unrelaxed structures. Notice the magnified scale.

$d_2 = z_{\text{F}} - z_{\text{Ca}}$, and with ϵ_1 and ϵ_2 the two static dielectric constants involved, we will obtain

$$\Delta V = \frac{4\pi}{A} \left(+ \frac{e_{\text{Si}}^*}{\epsilon_1} d_1 - \frac{e_{\text{F}}^*}{\epsilon_2} d_2 \right), \quad (2)$$

where we have assumed that $e_{\text{Ca}}^* = -e_{\text{F}}^* - e_{\text{Si}}^*$.

The sign of the VBO is therefore dependent not only on the effective charges involved, but also on d_1 and d_2 and, hence, on the interface morphology. For example, in a type *B* unrelaxed structure, the Ca⁺-F⁻ dipole layer prevails upon the Ca⁺-Si⁻ one, whereas in the relaxed one, the situation is opposite, due to the much larger Ca⁺-Si⁻ distance. In fact, from Table I, it is possible to note that going from the unrelaxed to the relaxed structure, the Ca-F distance remains almost unchanged ($\approx 8\%$ difference) while the Si₁^{sub}-Ca distance increases by as much as 20%.

In order to check the validity of this simple model, we have performed FLAPW calculations for some type *B* unit cells, in which only one atom of the interface region has been displaced with respect to its equilibrium position. The relevant structural parameters are reported in Table III. Note that the displacement of an atom by a quantity *u* leads to a

TABLE III. Structural parameters (in Å) and valence-band offset (in eV) for the structures obtained by the displacement of one of the interface atoms from its equilibrium position, compared with the VBO of the equilibrium structure.

	$d_1 = z_{\text{Ca}} - z_{\text{Si}_1^{\text{sub}}}$	u_1	$d_2 = z_{\text{F}} - z_{\text{Ca}}$	u_2	ΔV
Equilibrium	2.307		1.021		+0.67
F atom displacement	2.307		1.099	+0.078	+0.28
Ca atom displacement	2.385	+0.078	0.943	-0.078	+1.14
Si_1^{sub} atom displacement	2.229	-0.078	1.021		+0.57

distance d between the two charged planes, $d = d_{\text{eq}} + u$. By convention, a positive u always increases the distance between the charged planes [for example, a positive u_1 increases the distance d_1 between the Si_1^{sub} (-) and the Ca (+) charged planes, whereas a negative u_2 decreases the distance d_2 between the Ca (+) and the F (-) charged planes].

According to our simple electrostatic model, a decrease of d_1 leads to a smaller contribution of the Si-Ca dipole layer and, hence, to smaller VBO [see the structure in which the Si (-) atom is displaced]. Analogously, an increase of d_2 leads to a smaller offset, as shown by the structure in which the F atom is displaced. Therefore, when the Ca atom is displaced toward the F atom (so that d_1 increases, d_2 decreases), the changes of the two competing dipoles sum up and the offset raises consequently.

We now denote the potential lineup for the equilibrium and displaced positions by ΔV^{eq} and ΔV^{disp} , respectively. Using Eq. (2) the change of the VBO can be expressed as

$$\Delta(\Delta E_v) = \Delta V^{\text{disp}} - \Delta V^{\text{eq}} = \frac{4\pi}{A} \left(+ \frac{e_{\text{Si}}^*}{\varepsilon_1} u_1 - \frac{e_{\text{F}}^*}{\varepsilon_2} u_2 \right). \quad (3)$$

From Eq. (3), we could therefore derive the value of the Born effective charges ($e_{\text{Si}_1^{\text{sub}}}^*$, e_{Ca}^* , and e_{F}^*), provided that the values of the dielectric constants are known. The values of ε_1 and ε_2 to be considered are not the bulk ones of Si or CaF_2 , but they are a sort of local average between the dielectric constants involved.⁵ As a first approximation, we have considered an average dielectric constant ε_{ave} :

$$\frac{1}{\varepsilon_{\text{ave}}} = \frac{1}{2} \left(\frac{1}{\varepsilon_{\text{Si}}^{\text{expt}}} + \frac{1}{\varepsilon_{\text{CaF}_2}^{\text{expt}}} \right) \quad (4)$$

so that $\varepsilon_1 = \varepsilon_2 = \varepsilon_{\text{ave}}$. Using the experimental values $\varepsilon_{\text{Si}}^{\text{expt}} \approx 12$ and $\varepsilon_{\text{CaF}_2}^{\text{expt}} \approx 7.35$,⁹ we find $\varepsilon_{\text{ave}} = 9.2$. If we substitute in Eq. (3), $\varepsilon_1 = \varepsilon_2 = \varepsilon_{\text{ave}}$, u_1 and u_2 as reported in Table III, we find $e_{\text{F}}^* = -0.8$ and $e_{\text{Si}_1^{\text{sub}}}^* = -0.2$, so that $e_{\text{Ca}}^* = -(e_{\text{F}}^* + e_{\text{Si}_1^{\text{sub}}}^*) = 1$. The F dynamical charge looks therefore close to the nominal charge state of the ion: this is quite reasonable for a strongly ionic bond.

Let us now compare our results with the available experimental results of Dell'Orto *et al.*⁹ obtained from XPS measurements for an (a-Si)-Si(111) homojunction with a CaF

intralayer ($\Delta V_{\text{exp}} = -0.35$ eV). They found that the overlayer valence-band maximum is at lower binding energy with respect to the substrate one (and therefore a negative VBO, according to our convention), leading to an electrostatic dipole directed from the overlayer to the substrate. This seems to be at variance with several structures considered in this work (see Table II): one has to bear in mind that the interface formation is dominated by kinetics, and the minimum-energy ideal structure most often is not the one that really grows. Furthermore, the experimental system differs substantially from the model structures considered in the present work: the Si overlayer is constituted by amorphous Si, while we considered a perfect Si [111] ordered crystal at both sides of the homojunction (whose dangling bonds at the F side are saturated with H). The H content of the experimental amorphous overlayer and the detailed interface morphology are, of course, not known. We also recall that amorphous Si experimentally grown on the CaF intralayer could contain a variety of different types of atomic coordinations and bond lengths, all affecting the final VBO value. As already pointed out, our results show that the charge redistribution at the interface (and hence the band lineup) is crucially dependent on the interface morphology. Therefore, the disagreement between the experimental ($\Delta V_{\text{expt}} = -0.35$ eV) and theoretical (see Table II) VBO values is not surprising, and certainly due to the differences between the experimental and the simulated structures: we should remark that the experimental paper emphasizes the unpredictability of the detailed interface morphology, given the growth temperature of 500 °C–600 °C. A meaningful comparison between theory and experiment would thus require a precise knowledge of the interface morphology for this kind of very polar system.

V. CONCLUSIONS

FLAPW calculations performed for Si/CaFH/Si superlattices with different structural ordering (type A and type B) and bond lengths (unrelaxed and relaxed structures) show that the VBO, related to the charge readjustment at the interface, is strongly dependent on the interface morphology. In particular, for the unrelaxed structures, the interaction between the F and overlayer Si (and H) atoms in type B interfaces determines a charge flow from the F to the inner Si-Si bonds that is responsible for the appreciable change of the VBO. Moreover, our calculations show that the clean relaxed Si-Ca-F-H-Si interface has a dipole moment oriented from

the Si substrate toward the overlayer, resulting in higher binding energy for core levels belonging to the overlayer. The only experiment to compare with refers to an overlayer of amorphous Si, whose H content is unknown but presumably small, and indicates a dipole oriented in the opposite direction. The discrepancy is certainly related to the real in-

terface morphology, which is probably very complex and contains a variety of different structural orderings and atomic distances, leading to a potential lineup varying within a very large range (about 1.5 eV). Our theoretical range brackets the only available experimental figure.⁹ We predict a strong dependence of the measured effect on growth conditions.

-
- *Present address: INFM, Dipartimento di Fisica, Università degli Studi di L'Aquila, 67010 Coppito, L'Aquila, Italy.
- ¹P. Perfetti, C. Quaresima, C. Coluzza, C. Fortunato, and G. Margaritondo, *Phys. Rev. Lett.* **57**, 2065 (1986).
- ²D. W. Niles, M. Tang, J. McKinley, R. Zannoni, and G. Margaritondo, *Phys. Rev. B* **38**, 10 949 (1988).
- ³S. Baroni, R. Resta, A. Baldereschi, and M. Peressi, in *Spectroscopy of Semiconductor Heterojunctions*, Vol. 206 of *NATO Advanced Studies Institute Series B: Physics*, edited by G. Fasol, A. Fasolino, and P. Lugli (Plenum, New York, 1989), p. 251.
- ⁴L. Sorba, G. Bratina, G. Ceccone, A. Antonini, J.F. Walker, M. Micovic, and A. Franciosi, *Phys. Rev. B* **43**, 2450 (1991).
- ⁵M. Peressi, S. Baroni, R. Resta, and A. Baldereschi, *Phys. Rev. B* **43**, 7347 (1991).
- ⁶A. Baldereschi, M. Peressi, S. Baroni, and R. Resta, in *Proceedings of the International School of Physics "Enrico Fermi," Course CXVII, Semiconductor Superlattices and Interfaces*, edited by L. Miglio and A. Stella (Plenum, New York, 1993), p. 59.
- ⁷J. T. McKinley, Y. Hwu, B. E. C. Koltenbach, G. Margaritondo, S. Baroni, and R. Resta, *J. Vac. Sci. Technol. A* **9**, 917 (1991).
- ⁸M. Marsi, G. De Stasio, and G. Margaritondo, *J. Appl. Phys.* **72**, 1443 (1992).
- ⁹T. dell'Orto, G. De Stasio, M. Capozzi, C. Ottaviani, C. Quaresima, and P. Perfetti, *Phys. Rev. B* **48**, 8823 (1993).
- ¹⁰S. Satpathy and R. M. Martin, *Phys. Rev. B* **39**, 8494 (1989).
- ¹¹S. Ossicini, C. Arcangeli, and O. Bisi, *Phys. Rev. B* **43**, 9823 (1991).
- ¹²S. Ossicini, A. Fasolino, and F. Bernardini, *Phys. Rev. Lett.* **72**, 1044 (1994).
- ¹³M. A. Olmstead, R. I. G. Uhrberg, R. D. Bringans, and R. Z. Bachrach, *Phys. Rev. B* **35**, 7526 (1987).
- ¹⁴R. M. Tromp and M. C. Reuter, *Phys. Rev. Lett.* **61**, 1756 (1988).
- ¹⁵C. A. Lucas, G. C. Wong, and D. Loretto, *Phys. Rev. Lett.* **70**, 1826 (1993).
- ¹⁶T. Nakayama, M. Katayama, G. Selva, and M. Aono, *Phys. Rev. Lett.* **72**, 1718 (1994).
- ¹⁷S. Shinaroy, *Thin Solid Films* **187**, 231 (1990).
- ¹⁸H. J. F. Jansen and A. J. Freeman, *Phys. Rev. B* **30**, 561 (1984); E. Wimmer, H. Krakauer, M. Weinert, and A. J. Freeman, *Phys. Rev. B* **24**, 864 (1981).
- ¹⁹L. Hedin and B. I. Lundqvist, *J. Phys. C* **4**, 2064 (1971).
- ²⁰D. J. Chadi and M. L. Cohen, *Phys. Rev. B* **8**, 5747 (1973).
- ²¹Rici Yu, D. Singh and H. Krakauer, *Phys. Rev. B* **43**, 6411 (1991).
- ²²A. Di Pomponio, A. Continenza, R. Podloucky, and J. Vackár, *Phys. Rev. B* **53**, 9505 (1996).
- ²³J. Zegenhagen and J. R. Patel, *Phys. Rev. B* **41**, 5315 (1990).
- ²⁴S. Massidda, B. I. Min, and A. J. Freeman, *Phys. Rev. B* **35**, 9871 (1987).
- ²⁵Su-Huai Wei and Alex Zunger, *Phys. Rev. B* **52**, 12 039 (1995).
- ²⁶S. Picozzi, A. Continenza, and A. J. Freeman, *Phys. Rev. B* **53**, 10 852 (1996).
- ²⁷C. Ohler *et al.*, *Phys. Rev. B* **50**, 7833 (1994).
- ²⁸A. Continenza, S. Massidda, and A. J. Freeman, *Phys. Rev. B* **42**, 3469 (1990).
- ²⁹A. Baldereschi, S. Baroni, and R. Resta, *Phys. Rev. Lett.* **61**, 734 (1988).